



CrossMark
 click for updates

Cite this: *RSC Adv.*, 2016, 6, 68005

Effects of Fe(II) on microbial communities, nitrogen transformation pathways and iron cycling in the anammox process: kinetics, quantitative molecular mechanism and metagenomic analysis†

Duntao Shu,^{‡ab} Yanling He,^{*c} Hong Yue^{‡d} and Shucheng Yang^{*e}

Appropriate Fe(II) concentration has been regarded as a significant factor for fast start-up of the anammox (anaerobic ammonium oxidizing) process. However, little is known about the influences of Fe(II) on microbial communities, nitrogen transformation pathways and iron cycling in anammox systems. Moreover, detailed evidence for a “*Ca. Brocadia sinica*” growth rate under different levels of Fe(II) constraints remains unclear. In this study, results showed that with the increase of Fe(II) concentrations from 0.02 mM to 0.08 mM, the specific growth rate of anammox increased from 0.1787 d⁻¹ to 0.2648 d⁻¹. However, further increasing Fe(II) concentration to 0.12 mM slightly decreased the specific anammox growth rate to 0.2210 d⁻¹. The results of this study indicated that lower Fe(II) concentrations (0.06–0.08 mM) could significantly increase the anammox growth rate up to 0.2648 d⁻¹. In addition, the activity of anammox bacteria could be suppressed by higher Fe(II) concentrations (>0.08 mM). Quantitative molecular analyses showed that (AOA *amoA* + AOB *amoA*)/anammox, (AOA *amoA* + AOB *amoA* + anammox + *nrfA*)/bacteria, *nosZ*/(*nirS* + *nirK*), FeOB (iron oxidizing bacteria), and FeRB (iron reducing bacteria) were the key functional groups determining nitrogen loss. Furthermore, MiSeq sequencing indicated that *Chloroflexi*, *Proteobacteria*, *Planctomycetes*, and *Chlorobi* were the dominant phyla. In addition, 55.5% of generalists were identified as 9 functional groups. Correlation-based network analysis demonstrated that nitrogen-cycling-related functional genes had strong ecological inter-correlations with iron-cycling-related bacteria. Overall, combined analyses clearly revealed that the coupling of nitrification, anammox, DNRA (Dissimilatory nitrate reduction to ammonium), NAFO (Nitrate-dependent ferrous iron oxidation) and Feammox (Anaerobic ammonium oxidation coupled with ferric iron reduction) is a potential important pathway accounting for nitrogen loss in the anammox process under Fe(II) stress conditions.

Received 10th April 2016

Accepted 5th July 2016

DOI: 10.1039/c6ra09209h

www.rsc.org/advances

1. Introduction

Understanding of the microbial nitrogen cycle has been radically altered by the discovery of anaerobic ammonium oxidizing

(anammox) bacteria.¹ Anammox bacteria, which were discovered in a denitrifying bioreactor in the late 1980s, have the metabolic capacity to couple ammonium with nitrite to form N₂.² As an anaerobic and chemoautotrophic bacteria, anammox bacteria are affiliated with a monophyletic group in the phylum *Planctomycetes*, and the order *Brocadiales*.³ To date, six anammox bacteria genera have been proposed using 16S and 23S rRNA gene sequencing,^{4,5} and include “*Candidatus Brocadia*”, “*Ca. Anammoxoglobus*”, “*Ca. Jettenia*”, “*Ca. Kuenenia*”, “*Ca. Scalindua*”, and “*Ca. Anammoximicrobium*”. Due to being cost-effective and energy-efficient, anammox-related nitrogen removing technologies are currently applied in almost 100 full-scale wastewater treatment plants for treating ammonium rich industrial and municipal wastewaters with low COD/N ratios.^{6,7}

Despite the advantages of anammox-related technologies, the low growth rate and low cellular yield of anammox bacteria has been considered main obstacles for the application of mainstream and side-stream anammox processes.^{7,8} Therefore, establishing a rapid and successful start-up of the anammox-

^aCenter for Mitochondrial Biology and Medicine, The Key Laboratory of Biomedical Information Engineering of the Ministry of Education, School of Life Science and Technology, Xi'an Jiaotong University, Shaanxi 710049, China

^bState Key Laboratory of Crop Stress Biology in Arid Areas, College of Life Sciences, Northwest A&F University, Yangling, Shaanxi 712100, China

^cSchool of Human Settlements & Civil Engineering, Xi'an Jiaotong University, Shaanxi 710049, China. E-mail: heyl@mail.xjtu.edu.cn; Fax: +86 029 83395128; Tel: +86 029 83395128

^dState Key Laboratory of Crop Stress Biology in Arid Areas, College of Agronomy and Yangling Branch of China Wheat Improvement Center, Northwest A&F University, Yangling, Shaanxi 712100, China

^eSchool of Energy and Power Engineering, Xi'an Jiaotong University, Shaanxi 710049, China

† Electronic supplementary information (ESI) available. See DOI: 10.1039/c6ra09209h

‡ These authors contributed equally to this work.

based processes remains an important challenge. Currently, many strategies have been developed to promote the anammox cellular yield and to further establish a reliable anammox-based process. These include Fe(II) addition,^{9,10} Fe(III) addition,^{11,12} zero-valent iron and ferrous oxide,¹³ wash-out methods,^{14,15} ultrasound field,¹⁶ electric field,¹⁷ PVA-SA gel immobilization,¹⁸ and polyethylene glycol immobilization,¹⁹ which. In addition, previous studies have reported that addition of sequential bio-catalyst (anammox granules)²⁰ and inoculation of mature anammox granules²¹ could efficiently kick-start anammox-based systems. Although these studies indicated that anammox bacteria may have relatively higher activity, only Liu *et al.* suggested that 0.09 mM Fe(II) significantly enhanced the specific anammox growth rate up to 0.172 d⁻¹ (ref. 9) using a 300 ml anammox reactor with mixed anammox cultures. However, a detailed analysis of “*Ca. Brocadia sinica*” growth rate under different Fe(II) constraints has not been conducted.

Iron (Fe) is a potential energy source and an essential nutrient for anammox bacteria. In microbes, iron cycling is catalyzed by iron oxidizing bacteria (FeOB) and iron reducing bacteria (FeRB), which play pivotal roles in global nitrogen and iron cycling. Previous studies have reported that nitrate-dependent ferrous iron oxidation (termed as “NAFO”) is a potential pathway for nitrogen removal in anammox²² and denitrifying systems.²³ Moreover, a few studies have reported that anaerobic ammonium oxidation coupled with ferric iron reduction (termed as Feammox) contribute to nitrogen removal in wetlands and paddy soils.^{24,25} In addition, previous studies found that “*Ca. Kuenenia stuttgartiensis*” could have the potential to reduce ferric iron during anaerobic respiration.^{26,27} However, little is known about the role of FeOB and FeRB in anammox system with “*Ca. Brocadia sinica*” under different Fe(II) stress conditions.

In addition, the microbial structures in anammox system have been explored using various molecular biology methods such as clone library of 16S rRNA gene library, denaturing gradient gel electrophoresis (DGGE) analysis and fluorescence *in situ* hybridization (FISH). With the recent development of next-generation sequencing, high-throughput sequencing has received great attention. To date, metagenomic methods have been applied to investigate the microbial structures in full-scale wastewater treatment plants.^{28,29} In addition, 454 pyrosequencing³⁰ and illumina high-throughput sequencing³¹ have also been used on lab-scale and pilot-scale anammox systems.^{32,33} Knowledge on the microbial community structures and the links to the different Fe(II) stresses is therefore essential for the quick establishment of the stable anammox-based systems.

Furthermore, several 16S rRNA and functional genes, including FeOB 16S rRNA (*Acidimicrobium* spp. and *Ferrovum myxofaciens*), FeRB 16S rRNA (*Albidiferax ferrireducens*, *Geobacter* spp., and *Acidiphilium* spp.) anammox 16S rRNA, archaea ammonia monooxygenase (AOA-*amoA*), ammonia monooxygenase (AOB-*amoA*), nitrite oxidoreductase (*nxrA*), periplasmic nitrate reductase (*napA*) and membrane-bound nitrate reductase (*narG*), dissimilatory nitrate reductase (*nrfA*), copper-containing nitrite reductase (*nirK*), nitrite reductase (*nirS*), and

nitrous oxide reductase (*nosZ*),^{34–36} have been shown to play key roles in global nitrogen and iron cycling. Nevertheless, little is known about the taxonomical and functional microbial community dynamics under Fe(II) constraints, and the long-term effect of Fe(II) on these genes.

The present study is the first to investigate the microbial community structures dynamics and quantitative molecular mechanism of nitrogen transformation in anammox system under different Fe(II) stress conditions. Given the above arguments, the present study has following objectives: (1) to systematically evaluate the effects of Fe(II) stress on the specific anammox growth activity and long-term treatment performance of nitrogen removal; (2) to quantify the absolute gene copy numbers of the 16S rRNA and functional genes, and to determine the key functional gene groups under different Fe(II) constraints; (3) to explore the taxonomical and microbial community structure dynamics in an anammox system; (4) to reveal the co-occurrence patterns of bacterial communities and functional generalists.

2. Methods

2.1. Batch tests for kinetic evaluation and long-term performance of anammox bioreactor under Fe(II) addition

Anammox biomass in this study was obtained from a laboratory-scale sequencing batch reactor (SBR), which has been operated for more than 18 months with hydraulic retention time (HRT), influent NH₄⁺-N, and NO₂⁻-N concentrations were 4 h, 200 mg L⁻¹ and 220 mg L⁻¹, respectively. The removal efficiencies of NH₄⁺-N and NO₂⁻-N were 93.7% ± 0.2% and 95.8% ± 0.3%, respectively. In addition, the nitrogen removal rate was approximately 2.51 kg-TN (total nitrogen) per m³ per d. The dominant phyla detected in this anammox-SBR system was “*Ca. Brocadia sinica*” according to a previously study.³⁷

Prior to the adding Fe(II) into the vials, enriched anammox biomass were washed with 0.9% NaCl solution until NH₄⁺-N and NO₂⁻-N concentrations were undetectable. Then the anammox biomass was centrifuged at 12 000 rpm for 15 min and the supernatant was discarded. After that, the biomass pellet was re-suspended in nitrogen-free mineral medium (7.3 ± 0.2). For subsequent batch experiments, 10 ml of biomass pellet was dispensed in 100 ml serum glass vials sealed with silicon-teflon gaskets and polypropylene caps.³⁷ Then, an equal volume of NH₄⁺-N and NO₂⁻-N but with different Fe(II) concentrations (details in Table 1) were injected into the vials with a syringe. Then, the nitrogen-free mineral medium was added to a final volume of 60 ml. The final concentration of mixed liquor volatile suspended solids (MLVSS), NH₄⁺-N and NO₂⁻-N in each vial was 2850 mg L⁻¹, 115 mg L⁻¹ and 120 mg L⁻¹, respectively. These experimental procedures were performed in an anaerobic glove box. After doing so, all the experimental vials were incubated at 32 °C and shaken at a speed of 120 rpm in the dark. The water samples for further kinetic analysis were taken from the vials hourly over 8 h.

For kinetic evaluation, deviations between the measured NH₄⁺-N concentrations and the model predictions were

Table 1 Batch tests and long-term experiments conditions

	NH ₄ ⁺ -N (mg L ⁻¹)	NO ₂ ⁻ -N (mg L ⁻¹)	Fe(II) levels (mM)
Batch experiments			
Batch test 1	115	120	0.02
Batch test 2	115	120	0.04
Batch test 3	115	120	0.06
Batch test 4	115	120	0.08
Batch test 5	115	120	0.10
Batch test 6	115	120	0.12
Long-term experiments			
Seeding (0–27 days)	120	156	0
Phase I (28–46 days)	120	156	0.02
Phase II (47–64 days)	120	156	0.04
Phase III (65–82 days)	120	156	0.06
Phase IV (82–99 days)	120	156	0.08
Phase V (100–120 days)	120	156	0.10

measured by minimizing the sum of squares using the secant method embedded in AQUASIM 2.1 d.³⁸

In addition, Haldane substrate inhibition kinetics (eqn (1))³⁹ were conducted to explore the specific anammox activity (SAA) and specific anammox growth rates (μ_{AN}) under different Fe(II) stress conditions.

$$SAA = \frac{SAA_{max}}{1 + \frac{K_{Fe}}{S_{Fe}} + \frac{S_{Fe}}{K_I}} \text{ and } \mu_{AN} = \frac{\mu_{AN,max}}{1 + \frac{K_{Fe}}{S_{Fe}} + \frac{S_{Fe}}{K_I}} \quad (1)$$

where K_{Fe} is the half saturation constant; S_{Fe} is the Fe(II) concentration; K_I is the inhibition constant; SAA_{max} and $\mu_{AN,max}$ are the maximum specific anammox activity and specific anammox growth rates, respectively.

In long-term experiments, 1 L seeding sludge was taken from the above SBR reactor and incubated in a new SBR reactor, which had an effective volume of 2.6 L and operated under mesophilic conditions (32 ± 3 °C). This anammox reactor was constantly fed with 120 mg L⁻¹ NH₄⁺-N and 156 mg L⁻¹ NO₂⁻-N, as well as contained mineral medium and trace element solution.² The anammox SBR system was run in a 6 h-cycle, including a 10 min feeding period, 340 min anaerobic reaction with mechanical mixing (120 rpm), 20 min settling, and 10 min discharging of 1.5 L effluent. After 28 days of incubation, stock solution of Fe(II) was added into the anammox SBR system automatically at the end of each feeding period, which varied the levels of Fe(II) stress conditions (details in Table 1).

2.2. DNA extraction, PCR amplification and illumina MiSeq sequencing

At the end of each phase, 0.5 g anammox sludge samples were collected for DNA extraction using the FastDNA® SPIN Kit for Soil (Mp Biomedicals, Illkirch, France) according to the manufacturer's instructions. Genomic DNA concentrations were measured with Nanodrop Spectrophotometer ND-1000 (Thermo Fisher Scientific, USA) and its quality was checked in agarose gel (1.2%).

For PCR amplification of the hyper variable regions of V3–V4 region in the bacteria 16S rRNA gene, genomic DNA from each sample was amplified by PCR using the primer set 338F (5'-barcode-ACTCCTACGGGAGGCAGCAG-3') and 806R (5'-barcode-GGACTACHVGGGTWTCTAAT-3'). The PCR reaction and protocols were essentially as described by Shu *et al.*⁴⁰ Each PCR reaction was run in triplicate. Then, three independent PCR products were pooled in equal amounts and purified with Axy-Prep DNA Gel Extraction Kit (Axygen, USA) and quantified with a QuantiFluor™-ST (Promega, USA) according to the manufacturer's instructions. Finally, the amplicon libraries were constructed and run on a MiSeq illumina platform (300 bp paired-end reads) at Majorbio Bio-Pharm Technology Co., Ltd, (Shanghai, China). All original sequencing data have been archived at the National Center for Biotechnology Information (NCBI) Sequence Read Archive (SRA) database under the accession number SRR2770334.

2.3. Sequence processing and bioinformatics analysis

After sequencing, FLASH (Version 1.2.11, <http://www.ccb.jhu.edu/software/FLASH/>) was used to merge all raw paired-end sequences, and then trimomatic (Version 0.33, <http://www.usadellab.org/cms/?page=trimomatic>) was used to removal low quality reads, barcodes and primers. After filtration, the remaining high quality sequences were clustered into operational taxonomic units (OTUs) (97% similarity) using Usearch (Version 8.1, <http://www.drive5.com/usearch>). Then, the taxonomic classification was conducted using RDP classifier (Version 2.2, <http://www.sourceforge.net/projects/rdp-classifier/>) via Silva SSU database (Release 119, <http://www.arb-silva.de>) with a confidence threshold of 70%. Furthermore, based on these clusters, alpha diversity statistics including Chao 1 estimator, ACE estimator, Shannon index, Simpson index, Good's coverage, and rarefaction curves at a distance of 0.03, were calculated for five samples using the Mothur program (Version 1.30.1, http://www.mothur.org/wiki/Main_Page).

2.4. Quantitative real-time PCR

For better understanding of the “key players” in the nitrogen removal and its quantitative molecular mechanism in anammox process, qPCR was employed to explore the absolute abundance of bacterial 16S rRNA, anammox bacteria 16S rRNA, FeOB 16S rRNA, FeRB 16S rRNA and other functional genes (*i.e.* AOB-*amoA*, AOA-*amoA*, *nosZ*, *nirS*, *nirK*, *narG*, *napA*, and *nrjA*). These genes were quantified three times with Mastercycler ep realplex (Eppendorf, Hamburg, Germany) based on SYBR Green II method using previously described primers and protocols.⁴⁰ qPCR was performed in a 10 µl reaction mixture consisting of 5 µl SYBR® Premix Ex Taq™ II (Takara, Japan), 0.25 µl of each primer, 1 µl of genomic DNA and 3.5 µl dd H₂O. The amplification efficiencies of qPCR assays ranged from 95% to 110%, and R^2 value for each calibration curves exceeded 0.98. The C_t (threshold cycle) was used to calculated the copy numbers of all above mentioned genes.

2.5. Statistical and network analysis

Influent and effluent samples were collected on a daily basis and were analyzed immediately. The concentration of $\text{NH}_4^+\text{-N}$, $\text{NO}_2^-\text{-N}$, $\text{NO}_3^-\text{-N}$, and TN were determined based on standard methods.⁴¹ Stepwise regression analysis (SPSS 20, USA) was applied to evaluate the association between nitrogen transformation rates and the above mentioned functional genes. Furthermore, co-occurrence paired with the Spearman's correlation coefficient (ρ) > 0.6 or < -0.6 and P -value < 0.01 was considered statistically robust.⁴² Network analyses were conducted using R (Version 3.3, <https://www.r-project.org/>) with “vegan”, “igraph” and “Hmisc” packages in RStudio (Version 0.98, <https://www.rstudio.com/>).²⁸ Network visualization was performed on the Gephi platform (Version 0.91, <https://www.gephi.org/>).

3. Results and discussion

3.1. Batch experiments and kinetics evaluation

To investigate the $\text{NH}_4^+\text{-N}$ consumption profiles in six batch tests at different Fe(II) concentrations, the specific anammox growth rates were measured and the kinetics was fitted using secant method embedded in AQUASIM 2.1d.³⁸ As illustrated in Fig. 1a–f, the kinetics matched well with the corresponding experimental measurements. After an 8 h incubation, with increased levels of Fe(II) from 0.02 mM to 0.08 mM, the fitted specific anammox growth rates also showed a corresponding increase from 0.1787 d^{-1} to 0.2648 d^{-1} . However, it is found that the specific anammox growth rates decreased from 0.2648 d^{-1} to 0.2210 d^{-1} when Fe(II) concentrations increased from 0.08 mM to 0.12 mM. These results indicated that the highest specific anammox growth rate was 0.2648 d^{-1} in the presence of 0.08 mM Fe(II), which was 32.5% higher than that in batch test I. This indicated that lower Fe(II) concentrations (0.02–0.08 mM) may significantly promote the activity of anammox bacteria in accordance with previous studies,^{9,43} which reported that the anammox bacteria had the highest growth rate at 0.09 mM Fe(II). However, the activity of anammox bacteria could be suppressed under higher Fe(II) concentrations (>0.08 mM).

Additionally, as shown in Fig. 1g and h, the dependence of SAA and μ_{AN} on the Fe(II) concentration could be well described using the substrate inhibition kinetics model. Fitting results in Fig. 1 showed that the SAA_{max} and $\mu_{\text{AN,max}}$ were $0.10274\text{ kg NH}_4^+\text{-N per kg VSS per d}$ and 0.63028 d^{-1} , respectively. Meanwhile, as shown in Fig. 1g and h, 95% confidence interval was predicted further revealing that the specific anammox growth rate under Fe(II) stress conditions could be described by eqn (1).

Previous studies¹⁰ have reported that appropriate concentrations of Fe(II) (0.06–0.09 mM) could significantly improve the accumulation of Fe element inside anammox biomass, while higher Fe(II) (0.12–0.18 mM) concentrations had adverse effects on the accumulation of Fe element. Liu & Ni suggested that 0.09 mM Fe(II) significantly enhanced the specific anammox growth rate up to 0.172 d^{-1} compared to the control group.⁹ It was found that Fe(II) is an essential substrate for anammox bacteria and plays a pivotal role in the anammox

growth. There are two possible explanations for Fe(II) uptake by “*Ca. Brocadia sinica*”. First, “*Ca. Brocadia sinica*”, a Gram-negative anammox bacteria, possesses the Feo type of iron transport system. Feo-mediated system was thought to transport ATPase and was recognized to use ATP hydrolysis to energize Fe(II) uptake and anammox bacteria growth under iron-restricted conditions.⁴⁴ Second, it was found that Fe(II) played a key role in electron transport to generate cytochrome C, which is a key functional enzyme for the growth of anammox bacteria.⁴⁰ Thus, together with analysis from the SAA_{max} and $\mu_{\text{AN,max}}$ values, it is evident that lower Fe(II) concentrations (0.06–0.08 mM) could significantly promote the anammox growth rates and activities.

3.2. Treatment profiles and reactor performance

Long-term experiment in the anammox-SBR system for 120 days, revealed the nitrogen concentration, nitrogen removal efficiencies, nitrogen transformation rates, and nitrogen loading rates shown in Fig. 2. During the seeding phase without Fe(II) (1–28 days), the average $\text{NH}_4^+\text{-N}$, $\text{NO}_2^-\text{-N}$, and total nitrogen removal (TN) efficiencies were $91.76 \pm 0.97\%$, $98.64 \pm 0.14\%$, and $83.31 \pm 0.61\%$, respectively. Correspondingly, the nitrogen removal rate and nitrogen loading rate were 0.932 ± 0.010 and $1.119 \pm 0.009\text{ kg-N per m}^3\text{ per d}$, respectively. The average stoichiometric ratio of $\text{NH}_4^+\text{-N}$, $\text{NO}_2^-\text{-N}$, and $\text{NO}_3^-\text{-N}$ was $1 : (1.311 \pm 0.024) : (0.296 \pm 0.009)$, which was consistent with the theoretical values for anammox process.² During the phase I (29–46 days), the average $\text{NH}_4^+\text{-N}$, $\text{NO}_2^-\text{-N}$, and TN efficiencies were $92.476 \pm 0.79\%$, $99.218 \pm 0.152\%$, and $85.207 \pm 0.435\%$, respectively. Compared to the seeding phase, the average stoichiometric ratio of $\text{NH}_4^+\text{-N}$, $\text{NO}_2^-\text{-N}$, and $\text{NO}_3^-\text{-N}$ was $1 : (1.304 \pm 0.041) : (0.263 \pm 0.009)$. During the phase II (47–65 days), the Fe(II) concentration increased to 0.04 mM. As shown in Fig. 2, the average $\text{NH}_4^+\text{-N}$, $\text{NO}_2^-\text{-N}$, and TN efficiencies also increased slightly to $92.966 \pm 0.572\%$, $99.282 \pm 0.115\%$, and $85.947 \pm 0.341\%$, respectively. During the phase III (66–82 days), the average $\text{NH}_4^+\text{-N}$, $\text{NO}_2^-\text{-N}$, and TN efficiencies increased to $93.961 \pm 0.335\%$, $99.558 \pm 0.106\%$, and $87.202 \pm 0.296\%$, respectively. During the phase IV (83–102 days), the average $\text{NH}_4^+\text{-N}$, $\text{NO}_2^-\text{-N}$, and TN removal efficiencies had reached maximum values, which were $94.528 \pm 0.480\%$, $99.918 \pm 0.158\%$, and $88.893 \pm 0.985\%$, respectively. Furthermore, the average stoichiometric ratio of $\text{NH}_4^+\text{-N}$, $\text{NO}_2^-\text{-N}$, and $\text{NO}_3^-\text{-N}$ declined to $1 : (1.291 \pm 0.015) : (0.202 \pm 0.017)$. With an increase in Fe(II) concentrations from 0.08 mM to 0.10 mM, the average $\text{NH}_4^+\text{-N}$, $\text{NO}_2^-\text{-N}$, and TN removal efficiencies declined to $93.008 \pm 0.811\%$, $99.293 \pm 0.280\%$, and $85.928 \pm 0.682\%$, respectively. However, the average stoichiometric ratio of $\text{NH}_4^+\text{-N}$, $\text{NO}_2^-\text{-N}$, and $\text{NO}_3^-\text{-N}$ increased to $1 : (1.307 \pm 0.013) : (0.252 \pm 0.008)$ when compared to the ratio in phase IV.

In general, the results from the long-term treatment performance of anammox-SBR system under different Fe(II) constraints indicated that lower concentrations of Fe(II) (<0.08 mM) could significantly improve $\text{NH}_4^+\text{-N}$ and TN removal but it could be suppressed by higher Fe(II) concentrations (>0.10 mM), which was consistent with previous results.⁴³ In addition, in

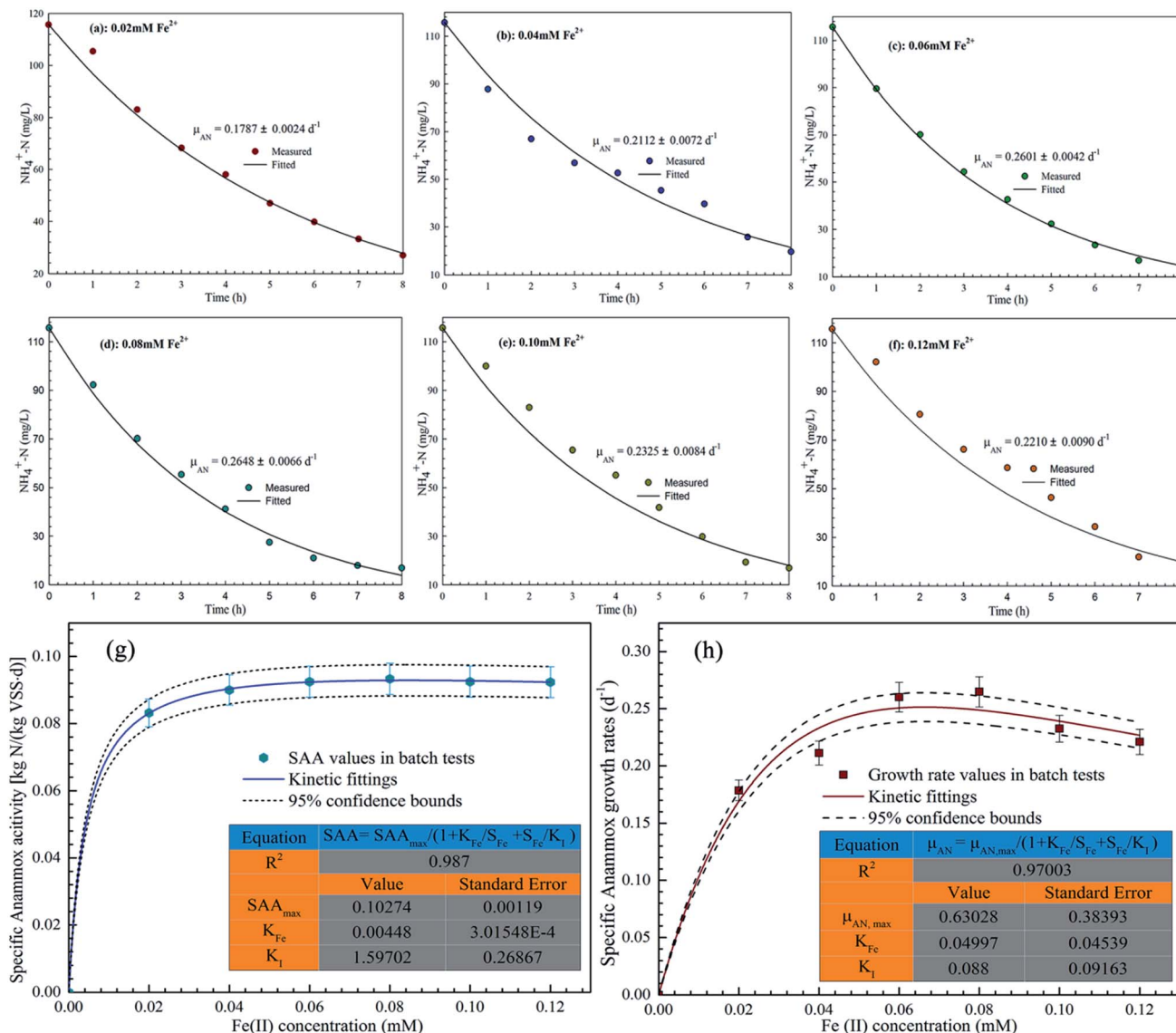


Fig. 1 (a–f) The kinetic fitted and measured NH_4^+-N consumption profiles in six 8 h batch tests under different $\text{Fe}(\text{II})$ conditions; (g) the actually observed and model-fitted relationships between $\text{Fe}(\text{II})$ conditions and specific anammox activity using substrate inhibition kinetics; (h) relationships between $\text{Fe}(\text{II})$ conditions and specific anammox growth rates.

comparison with the anammox growth rates in the batch tests, the tendency of nitrogen transformation rates during the entire experimental period was not significant. Furthermore, as described in Fig. 2d, although the average nitrogen stoichiometric ratio of $\Delta\text{NO}_2^-/\Delta\text{NH}_4^+$ during entire period stabilized at 1.3 ± 0.02 , the average stoichiometric ratio of $\Delta\text{NO}_3^-/\Delta\text{NH}_4^+$ declined from 0.30 ± 0.02 to 0.25 ± 0.02 . There are two possible explanations for these results. First, partial $\text{Fe}(\text{II})$ was utilized by the $\text{Fe}(\text{II})$ -oxidizer, such as reported for the *Acidovorax* strains.⁴⁵ Second, microbial processes other than anammox, such as nitrate-dependent $\text{Fe}(\text{II})$ oxidation and ferric ammonium oxidation could greatly contribute to nitrogen removal in this study. These results are accordant with previous studies, indicating that “*Ca. Brocadia sinica*” likely oxidized $\text{Fe}(\text{II})$ with nitrate as an electron donor.²²

3.3. Quantification of 16S rRNA and functional genes

In order to gain insights into the influence of $\text{Fe}(\text{II})$ concentration on the nitrogen and iron-related functional genes, anammox biomass were taken from the end of each phase and the copy numbers of all above mentioned 16S rRNA and functional genes were quantified. As shown in Fig. 3a, during the four phases (phase I–IV), the absolute abundance of 16S rRNA increased marginally from 1.12×10^9 to 2.00×10^9 copies per (g wet sludge) with an increase in $\text{Fe}(\text{II})$ levels from 0.02 mM to 0.08 mM. However, the gene copy numbers of anammox 16S rRNA slightly decreased in the phase V. This result was consistent with the specific anammox growth rates in batch experiments. It was evident that higher $\text{Fe}(\text{II})$ concentrations (>0.10 mM) could decrease the activity of anammox 16S rRNA.

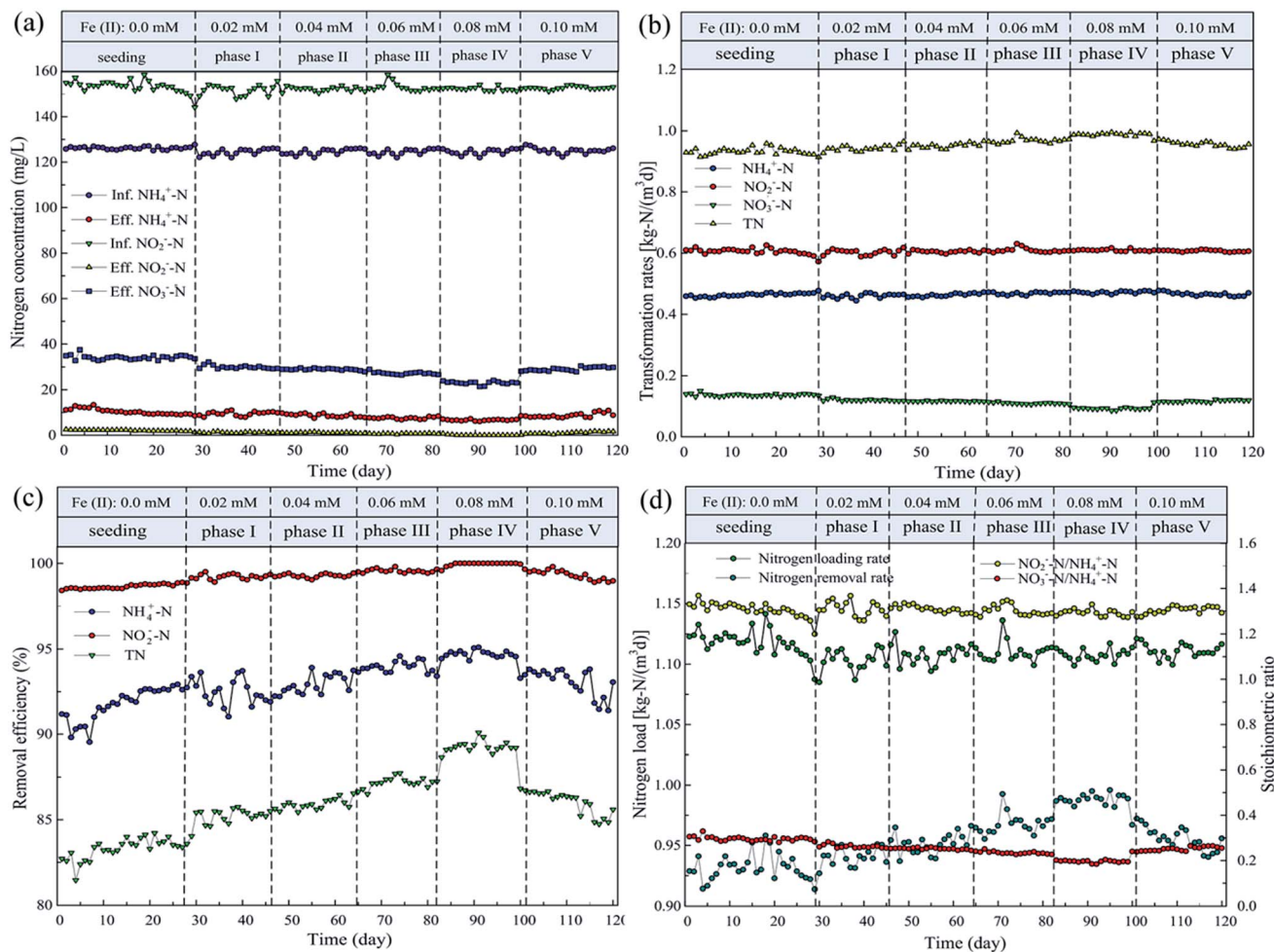


Fig. 2 Long term performance of anammox reactor under different Fe(II) conditions (a) concentration; (b) removal efficiency; (c) transformation rates; (d) nitrogen load.

The absolute abundance of three nitrification genes, AOA *amoA*, AOB *amoA* and *nxrA* genes is presented in Fig. 3b. The gene copy numbers of AOB *amoA* during the entire experimental period were 1–3 orders of magnitude higher than AOA *amoA* and *nxrA* genes. In addition, the gene copy numbers of *nxrA* gradually declined with an increase in Fe(II) concentrations increased from 0.02 mM to 0.08 mM. However, as shown in Fig. 3b, 0.10 mM Fe(II) increased the *nxrA* gene copy numbers. These results indicated that the conversion of $\text{NO}_2^-\text{-N}$ to $\text{NO}_3^-\text{-N}$ could be inhibited by the lower Fe(II) concentrations.

As illustrated in Fig. 3c, the gene copy numbers of dissimilatory nitrogen reduction genes, *napA* and *narG*, slightly declined during all five phases. However, the gene copy numbers of *nrFA* gene increased from 5.39×10^4 to 9.06×10^4 copies per (g wet sludge) during phases I–IV along with an increase in Fe(II) concentration from 0.02 to 0.08 mM. In addition, the gene copy numbers of *nrFA* in phase IV were three times more than in phase V. Notably, the variations of *nrFA* and anammox gene copy numbers had a high degree of consistency, indicating that combining DNRA and anammox⁴⁶ may have significantly contribution to nitrogen removal in the presence of appropriate Fe(II) concentrations. As shown in Fig. 3d, the gene

copy numbers of *nirS* involved in denitrification were more abundant than *nirK* and *nosZ* genes. In addition, the gene copy numbers of *nirK*, *nirS* and *nosZ* from phase I–IV were nearly 0.9–1.2 orders of magnitude higher than that in the phase V. It appears that lower Fe(II) concentrations (0.02–0.08 mM) could slightly promote the activity of denitrify microorganisms.

FeOB genes, including *Acidimicrobium* and *Ferroplasma* 16S rRNA genes were displayed in Fig. 3e. The results showed that the *Acidimicrobium* and *Ferroplasma* 16S rRNA gene copy numbers were in the same order of magnitude from phase I–II, while the *Ferroplasma* 16S rRNA gene copy numbers were nearly 1–2 orders of magnitude higher than *Acidimicrobium* 16S rRNA gene copy numbers in the phase IV–V. These results also indicated that lower Fe(II) concentrations (0.02–0.04 mM) had no significant impact on FeOB group, while *Acidimicrobium* spp. could be inhibited by higher Fe(II) concentrations (0.06–0.10 mM). Furthermore, as shown in Fig. 3d, the gene copy numbers of *Geobacter* 16S rRNA varied marginally during the entire experimental period, while *Albidiferax* 16S rRNA and *Acidiphilium* 16S rRNA genes involved in FeRB group varied markedly. These results indicated that appropriate Fe(II) addition could be beneficial to the activity of *Geobacter* spp.

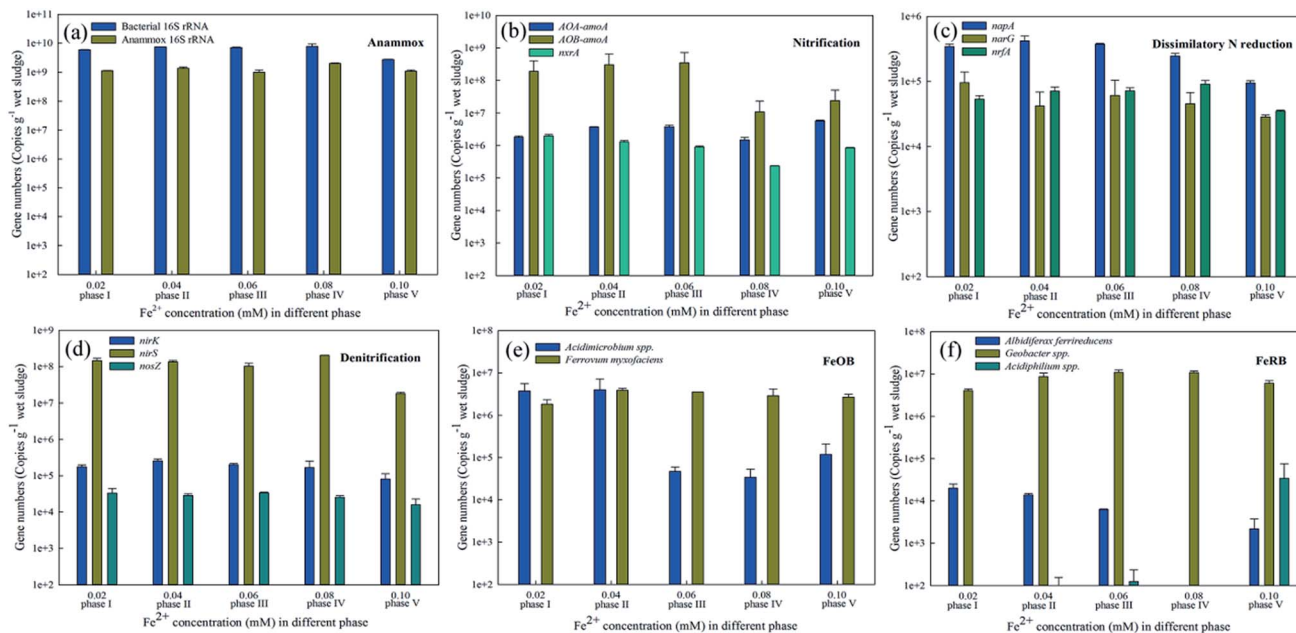


Fig. 3 Quantitative analysis of nitrogen and iron-cycling-related genes in the anammox system. Error bars represent standard deviation calculated from three independent experiments.

Taken together, it is plausible that an increase in Fe(II) concentration could result in a higher abundance of FeOB and FeRB. In addition, the results of qPCR showed that the *anammox*, *nrfA*, and *nirS* gene copy numbers increased during phase I–IV. Thus, it is evident that anammox, DNRA and denitrification could in part function alongside FeOB and FeRB suggested in previous studies.^{24,29}

3.4. Molecular mechanism of nitrogen transformation rates

To further elucidate the relative contributions of these functional genes to nitrogen removal in the presence of Fe(II), the quantitative molecular correlations between nitrogen transformation rates with these nitrogen and iron cycling related functional genes were performed. As shown in Table 2, four equations for $\text{NH}_4^+\text{-N}$, $\text{NO}_2^-\text{-N}$, $\text{NO}_3^-\text{-N}$, and TN were successfully established with R^2 values ranging from 0.982 to 0.998. The $\text{NH}_4^+\text{-N}$ transformation rate was jointly determined by four variables, including (AOA *amoA* + AOB *amoA*)/anammox, *nxrA*, AOB, and FeOB. Two variables (AOA *amoA* + AOB *amoA*)/anammox and AOB were denoted as $\text{NH}_4^+\text{-N}$ consumption, which showed positive correlation with $\text{NH}_4^+\text{-N}$ transformation. However, the *nxrA* and FeOB negatively correlated with $\text{NH}_4^+\text{-N}$ transformation. One explanation for this relationship could be that *nxrA* consumed $\text{NO}_2^-\text{-N}$ and produced $\text{NO}_3^-\text{-N}$. Therefore, the conversion pathway of $\text{NO}_2^-\text{-N}$ or $\text{NO}_3^-\text{-N}$ reduction to $\text{NH}_4^+\text{-N}$ could decline $\text{NH}_4^+\text{-N}$ consumption.

Furthermore, $\text{NO}_2^-\text{-N}$ transformation rate has negatively correlated with (AOA *amoA* + AOB *amoA* + anammox)/bacteria and *narG*. These two variables also showed negative associations with $\text{NO}_2^-\text{-N}$ accumulation. These correlations could exist likely because the process of ammonia oxidation, anammox and dissimilatory nitrate reduction were inhibited by the

accumulation of the metabolic product $\text{NO}_2^-\text{-N}$ under high concentrations.^{20,47}

In addition, $\text{NO}_3^-\text{-N}$ transformation rate was collectively determined by *nosZ*/(*nirS* + *nirK*), FeOB, and FeRB (Table 2). The variables *nosZ*/(*nirS* + *nirK*) and FeRB were denoted for $\text{NO}_3^-\text{-N}$ consumption and ferric iron reduction, respectively. These two variables showed negative relationship with the $\text{NO}_3^-\text{-N}$ transformation rate. However, the variable FeOB had a positive correlation with $\text{NO}_3^-\text{-N}$ transformation.

As displayed in eqn (2)–(4),⁴⁸ this relationship suggested that nitrate-dependent anaerobic ferrous oxidation (termed NAFO) contribution to $\text{NO}_3^-\text{-N}$ transformation.²²

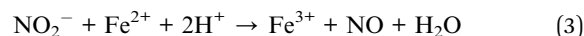
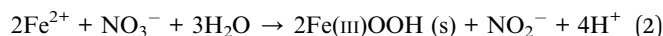
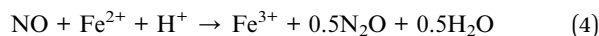
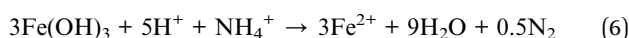
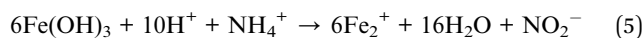


Table 2 Quantitative response relationships between nitrogen transformation rates ($\text{mg L}^{-1} \text{d}^{-1}$) and functional genes abundance (copies per g sludge) in long-term experiment ($n = 5$)

Stepwise regression models (equations)	R^2	P value
$\text{NH}_4^+\text{-N} = 0.004 \times (\text{AOA } amoA + \text{AOB } amoA)/\text{anammox} - 4.599 \times 10^{-10} \text{ } nxrA + 2.518 \times 10^{-12} \text{ AOB} - 1.222 \times 10^{-9} \text{ FeOB} + 0.477$	0.988	0.034
$\text{NO}_2^-\text{-N} = -0.05 \times (\text{AOA } amoA + \text{AOB } amoA + \text{anammox})/\text{bacteria} - 4.005 \times 10^{-7} \text{ } narG + 0.639$	0.982	0.025
$\text{NO}_3^-\text{-N} = -8.025 \times 10^{-14} \text{ bacteria} - 1.765 \times \text{ } nosZ/(\text{ } nirS + \text{ } nirK) + 1.294 \times 10^{-9} \text{ FeOB} - 2.805 \times 10^{-9} \text{ FeRB} + 0.131$	0.998	0.010
$\text{TN} = 0.089 \times (\text{AOA } amoA + \text{AOB } amoA + \text{anammox} + \text{ } nrfA)/\text{bacteria} + 6.138 \times 10^{-9} \text{ FeRB} + 0.890$	0.987	0.018



Additionally, as shown in eqn (5) and (6),²⁵ anaerobic ammonium oxidation can be coupled with ferric iron (Fe(III)) reduction (Feammox) to produce NO_2^- or N_2 through the following process.



As shown in Table 2, TN transformation rate was determined by (AOA *amoA* + AOB *amoA* + anammox + *nrfA*)/bacteria and FeRB, which indicated that not only did *amoA*, anammox and DNRA play pivotal roles in nitrogen removal, but ferric iron reduction (termed Feammox) was a significant microbial pathway for TN removal.²⁵

Taken together, quantitative molecular analyses indicated that the co-existence of nitrification, anammox, DNRA, NAFO and Feammox processes could be useful for the simultaneous removal of nitrogen, ferrous salt and ferric salt in industrial and municipal wastewater treatment.

3.5. Shifts of bacterial community and functional generalists

In this study, MiSeq high-throughput sequencing was applied to explore the effects of Fe(II) on bacterial communities and functional generalists in the anammox reactor. The results displayed that 1 2125–1 8283 clean reads were obtained from each sample after MiSeq sequencing (Table S3†). Based on the sequencing results, OTUs were in the range of 132–230, and 118 among the 805 OTUs were shared by all samples. Four estimators (Good's coverage, Shaanon, Chao 1, and ACE estimator) found no significant difference among the OTUs. However, Simpson estimator in phase IV was 1.85–3.71 times higher than the other four phases. These results indicated that Fe(II) did not significantly influence the richness of anammox biomass, although it could significantly enhance the diversity of bacteria throughout the entire experimental period. Additionally, as shown in Fig. S1,† more than 12 500 reads were obtained for each sample and the rarefaction curves reach a plateau without phase V, indicating that new species could not continue to emerge when sequence depth exceed 12 500.

In this study, effective sequences from each phase were assigned to phyla, classes, order, family, and genera. A total of 15 bacterial phyla across five phases were identified using RDP classifier combined with Silva SSU database at 70% threshold. Results from Fig. 4 showed that *Chloroflexi* was the most dominant phylum in all phases, accounting for 27.9–55.8% (averaging at 41.3%). The other dominant phyla were *Proteobacteria* (13.5–24.0%, averaging at 19.6%), *Planctomycetes* (13.6–20.9%, averaging at 18.6%), and *Chlorobi* (3.7–10.2%, averaging at 7.3%). These results are consistent with previous studies,³¹ showing that *Chloroflexi* and *Proteobacteria* were the most dominant phyla in nitrification–anammox reactors. Additionally, Fig. 4 clearly showed that *Proteobacteria* and *Chloroflexi* were more abundant in phase IV than in the remaining four phases. On one hand, it can be presumed that *Proteobacteria* and

Chloroflexi play key roles in nitrogen removal in the anammox bioreactor with Fe(II) addition. On the other hand, the diversity of *Proteobacteria* and *Chloroflexi* could be improved with appropriate Fe(II) levels. Among *Proteobacteria*, β -*Proteobacteria* (10.60–14.93%) was the most dominant in all phases, followed by α -*Proteobacteria* (1.49–4.33%), γ -*Proteobacteria* (0.87–3.28%), and δ -*Proteobacteria* (0.47–1.47%) (Fig. S2†). In addition, these four classes were shared by the four phases. Therefore, it can be concluded that these four classes could significantly contribute towards nitrogen removal during nitrogen and iron cycling, which is also in accordance with other studies.²⁹ Besides the classes, the following major orders (>1% at least one phase) (Fig. S2b and c†), including *Anaerolineales*, *Brocadiales*, *Rhodocyclales*, *Ignavibacteriales*, *Caldilineales*, *Phycisphaerales*, *Nitrosomonadales*, and *Cytophagales*, and their corresponding families were dominant populations and shared by five phases.

Among the effective sequences, 16 out of 36 genera were more dominant in four phases and accounted for 73.4–94.8% of the assigned genera (Fig. S2d†). Within these dominant genera, only 9 genera were commonly shared by four phases (>1% in any samples). These genera, including *Anaerolineaceae* (20.95–51.58%), *Candidatus Brocadia* (10.35–17.35%), and *Rhodocyclaceae* (4.77–8.60%), were considered to be the core and distinct genera in the anammox processes. It is noteworthy that *Candidatus Brocadia* was the dominant anammox population in this study. This genus is also the most abundant in the phylum, *Planctomycetes*. These results implicated the key roles of *Planctomycetes* and genus of *Candidatus Brocadia* in the anammox process, which was in agreement with previous studies.⁴⁹

Considering the significant roles of some nitrogen and iron-cycling-related bacterial groups in stabilizing the anammox process, it is reasonable to presume that these functional bacterial groups could have strong co-occurring associations.⁵⁰ To confirm this presumption, 36 dominant genera were selected and analyzed. Results shown in Fig. 5 revealed that 55.5% of generalists were identified as 9 functional groups, namely, one anammox bacteria, one AOB, seven chemo-organotrophic bacteria, four denitrifier, two fermenters, two NOB, one PAH degrading bacteria, one SOB, and other seventeen unassigned functional groups. These results indicated that Fe(II) could enhance the richness of bacteria. It should be noted that the abundance of *Candidatus Brocadia* and chemo-organotrophic bacteria can be increased with an increase in Fe(II) concentration from 0.02–0.08 mM. However, the abundance of denitrifier has been significantly improved with 0.10 mM of Fe(II) concentration. It can be concluded that while high concentration of Fe(II) could restrain the anammox bacteria, it could benefit denitrifier and NOB.

3.6. Network analysis of microbial co-occurrence patterns

To explore the ecological interactions between bacterial taxa, the network analysis of co-occurrence patterns was performed based on Spearman's coefficient >0.6 (<−0.6) and *P* value < 0.01.^{42,51} The results shown in Fig. 6a demonstrated that the positive network of anammox biomass has 39 nodes and 24 edges. In this study, some topological properties widely applied

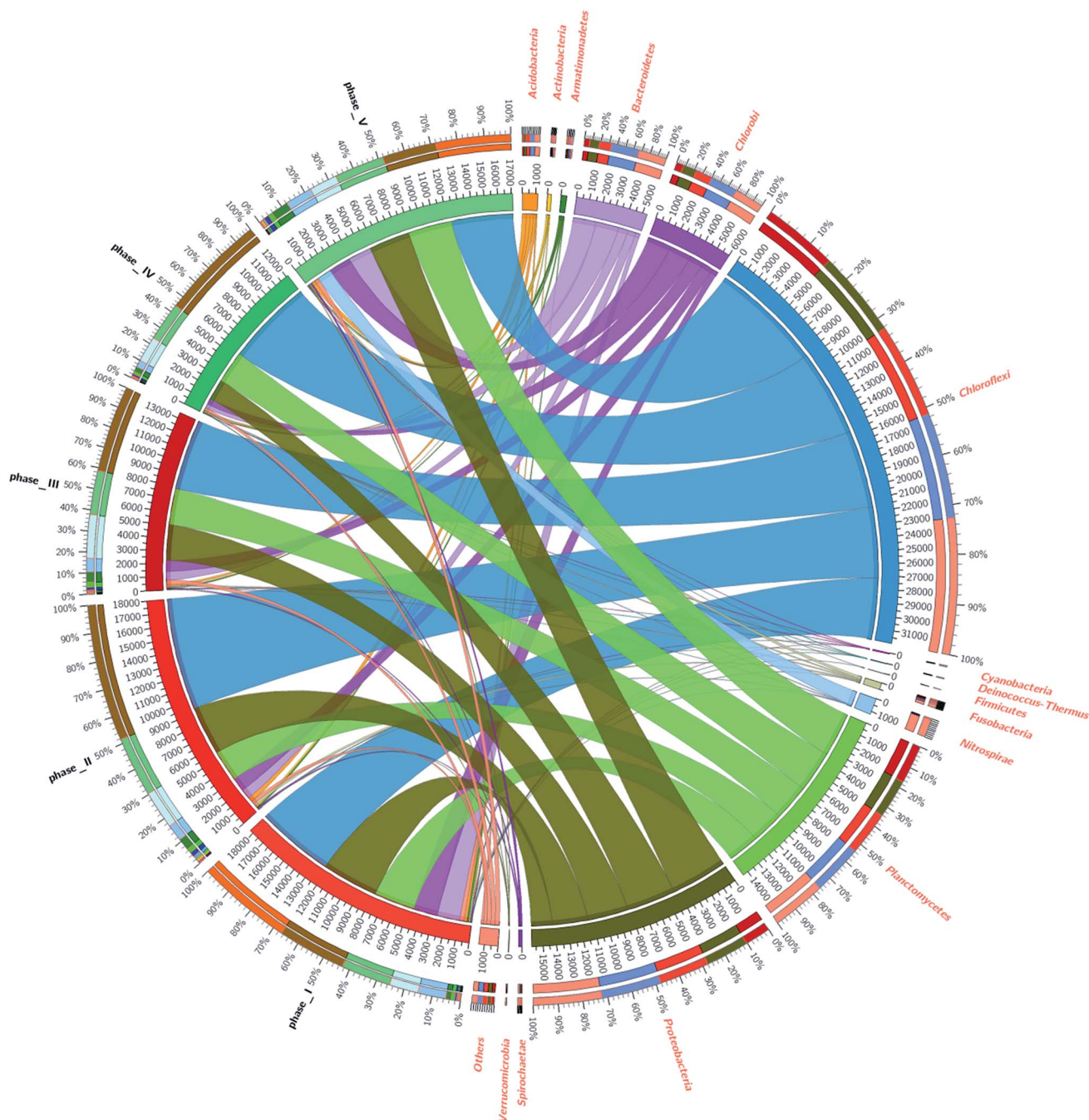


Fig. 4 Distribution of phyla in the different phase based on the taxonomy annotation from SILVA SSU database using QIIME pipeline. The thickness of each ribbon represents the abundance of each taxon. The absolute tick above the inner segment and the relative tick above the outer segment stand for the reads abundances and relative abundance of each taxon. Others refer to those unassigned reads. The data were visualized using Circos (Version 0.67, <http://www.circos.ca/>).

in this network analysis were measured to elucidate the complex pattern of the inter-correlations between functional genera.^{42,51} For this positive network, the average path length (APL) between nodes was 1 edge and the network diameter (ND) of 1 edge. In addition, the average clustering efficient (ACC) and modularity were 0.179 and 0.774, respectively. It was evident that this network had a modular structure and “small world” properties. Based on the phylum level, this network was parsed

into 10 phyla, with 10 among 39 total vertices occupied by the 8 dominant phyla. In this network, these densely connected nodes in each phylum were considered as the “hub” of network. As shown in Fig. 6a, it was found that *Bryobacter*, *Candidatus Brocadia*, *Ignavibacterium*, *Alistipes*, *Faecalibacterium*, and *Anaerolinea* were the hub of *Acidobacteria*, *Planctomycetes*, *Chlorobi*, *Bacteroidetes*, *Firmicutes*, and *Chloroflexi*, respectively. Based on the results of hub, *Planctomycetes* showed positive inter-



Fig. 5 The relative abundance of total 9 functional genera in the 5 samples.

correlation with *Proteobacteria*. In addition, *Chlorobi* showed positive inter-relationship with *Proteobacteria* and *Bacteroidetes*. There are two reasons to explain these hubs and related co-occurring genera. On one hand, these genera likely established a mutually symbiotic relationship in the anammox bioreactor in the presence of Fe(II). On the other hand, these hubs could be used as representatives of genera that act as the indicators of their corresponding phylum.

Furthermore, the co-occurrence patterns between bacterial diversity and functional genes diversity were also explored using network analysis. As displayed in Fig. 6b, the functional group consisted of 51 nodes and 21 edges. The observed APL (1.0), ND (1.0), and ACC (0.127) were calculated to describe the co-occurrence patterns between functional genes and bacterial taxa. The results in Fig. 6a showed that anammox bacteria,

FeOB, FeRB, and DNRA bacteria accounted for 3.92%, 3.92%, 5.88%, 1.96% of all functional group and bacterial taxa, respectively. In addition, *Candidatus Brocadia* was the hub of the anammox group. The denitrifier group consisted of *Comamonas*, *Pseudomonas*, *Steroidobacter*, *napA*, and *nirS* genes.

For the entire positive network, Fig. 6b also demonstrated that *Candidatus Brocadia* correlated positively with *napA* and *Albidiferax* spp., indicating that the mutualism of anammox bacteria, denitrifier and FeRB could be beneficial for the simultaneous removal of nitrogen and organic carbon.^{24,52} In addition, *nrfA* gene also correlated positively with *Limnobacter*. This result indicated that DNRA bacteria could use organic matter as the electron donors, which is in accordance with previous reports.^{53,54} Interestingly, the genus *Acidiphilium* in the

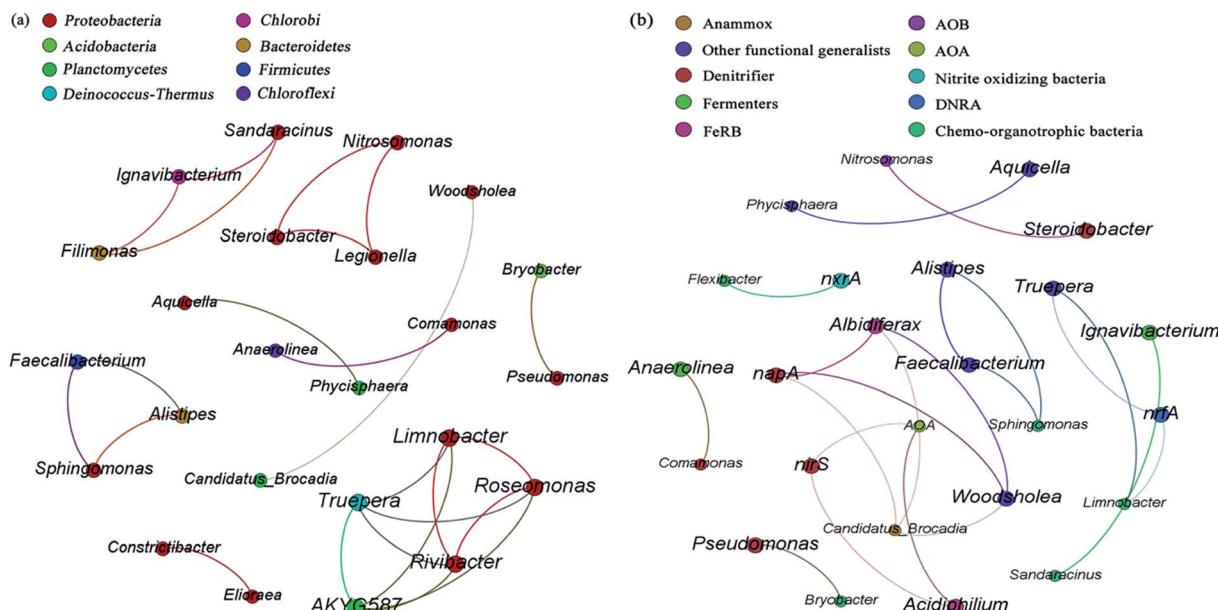


Fig. 6 Networks analysis of co-occurrence patterns for bacterial and functional generalists. A connection stands for a strong (Spearman's $\rho > 0.6$) and significant (P -value < 0.01) correlation. (a) Correlations between various genera with each node representing a bacterial genus and the color representing the phylum. (b) Correlations between various functional groups with each node representing a genus and the color representing the functional group.

FeRB group showed positive association with the AOA gene, indicating that the coupling of iron reduction and archaea ammonium oxidization could be useful for the removal of nitrogen in the nitrogen and iron cycling.

Overall, based on the network analysis from the results of the co-occurrence patterns, these findings are broadly consistent with the quantitative molecular analysis and provide novel insights into the inter-taxa correlations between microbial communities and functional genes in the anammox process. However, the co-occurrence associations revealed by network analysis in the organotrophic anammox need further investigation.

4. Conclusion

Batch tests and long-term experiments clearly demonstrated that anammox activity could be enhanced in the presence of appropriate Fe(II) concentration. Additionally, qPCR results and quantitative molecular analyses systemically confirmed that coupling of nitrification, anammox, DNRA, NAFO and Feammox was important pathway for nitrogen loss in the anammox process with Fe(II) addition. Results from the MiSeq high-throughput sequencing revealed that *Chloroflexi*, *Proteobacteria*, *Planctomycetes*, and *Chlorobi* were the most abundant phyla in all five phases. Furthermore, based on the results of microbial co-occurrence patterns, some nitrogen-cycling-related functional genes had strong ecological inter-correlations with iron-cycling-related bacteria. However, the quantitative molecular mechanism of Fe(III) reducing rate and oxidizing rate in anammox-SBR system needs further study using ^{15}N -labeled ammonium-based isotopic tracing

techniques. Moreover, the molecular mechanism for potential iron respiration in "*Ca. Brocadia sinica*" should also be further explored using metagenomic and metatranscriptomic approaches.

Acknowledgements

This study was financially supported by the National Natural Science Foundation of China (51308453) and Science & Technology Innovative Program of Shaanxi Province (2011KTZB03-03-01). The authors are grateful to Hong Yue for her assistance in equipment supply and network analysis. We sincerely appreciate Liang Zhu for kindly providing "*Ca. Brocadia sinica*" biomass.

References

- 1 A. Mulder, A. Graaf, L. Robertson and J. Kuenen, *FEMS Microbiol. Ecol.*, 1995, **16**, 177–184.
- 2 A. A. Van de Graaf, P. de Bruijn, L. A. Robertson, M. S. Jetten and J. G. Kuenen, *Microbiology*, 1996, **142**, 2187–2196.
- 3 M. Strous, J. G. Kuenen and M. S. Jetten, *Appl. Environ. Microbiol.*, 1999, **65**, 3248–3250.
- 4 J. G. Kuenen, *Nat. Rev. Microbiol.*, 2008, **6**, 320–326.
- 5 B. Kartal, L. van Niftrik, J. T. Keltjens, H. J. Op den Camp and M. S. Jetten, *Adv. Microb. Physiol.*, 2012, **60**, 212.
- 6 S. Lackner, E. M. Gilbert, S. E. Vlaeminck, A. Joss, H. Horn and M. van Loosdrecht, *Water Res.*, 2014, **55**, 292–303.
- 7 T. Lotti, R. Kleerebezem, J. Abelleira-Pereira, B. Abbas and M. van Loosdrecht, *Water Res.*, 2015, **81**, 261–268.

- 8 B. Kartal, N. M. Almeida, W. J. Maalcke, H. J. Camp, M. S. Jetten and J. T. Keltjens, *FEMS Microbiol. Rev.*, 2013, 1–34.
- 9 Y. Liu and B.-J. Ni, *Sci. Rep.*, 2015, 5, 8204.
- 10 S. Qiao, Z. Bi, J. Zhou, Y. Cheng and J. Zhang, *Bioresour. Technol.*, 2013, 142, 490–497.
- 11 H. Chen, J.-J. Yu, X.-Y. Jia and R.-C. Jin, *Chemosphere*, 2014, 117, 610–616.
- 12 S. Liu and H. Horn, *Bioresour. Technol.*, 2012, 114, 12–19.
- 13 F. Gao, H. Zhang, F. Yang, H. Li and R. Zhang, *Process Biochem.*, 2014, 49, 1970–1978.
- 14 M. Laurenzi, P. Falás, O. Robin, A. Wick, D. G. Weissbrodt, J. L. Nielsen, T. A. Ternes, E. Morgenroth and A. Joss, *Water Res.*, 2016, 101, 628–639.
- 15 H. Li, S. Zhou, W. Ma, G. Huang and B. Xu, *Desalination*, 2012, 286, 436–441.
- 16 X. Duan, J. Zhou, S. Qiao and H. Wei, *Bioresour. Technol.*, 2011, 102, 4290–4293.
- 17 X. Yin, S. Qiao and J. Zhou, *Appl. Microbiol. Biotechnol.*, 2015, 99, 6921–6930.
- 18 M. Ali, M. Oshiki, L. Rathnayake, S. Ishii, H. Satoh and S. Okabe, *Water Res.*, 2015, 79, 147–157.
- 19 K. Isaka, H. Itokawa, Y. Kimura, K. Noto and T. Murakami, *Bioresour. Technol.*, 2011, 102, 7720–7726.
- 20 C. J. Tang, P. Zheng, C. H. Wang, Q. Mahmood, J. Q. Zhang, X. G. Chen, L. Zhang and J. W. Chen, *Water Res.*, 2011, 45, 135–144.
- 21 S.-Q. Ni, B.-Y. Gao, C.-C. Wang, J.-G. Lin and S. Sung, *Bioresour. Technol.*, 2011, 102, 2448–2454.
- 22 M. Oshiki, S. Ishii, K. Yoshida, N. Fujii, M. Ishiguro, H. Satoh and S. Okabe, *Appl. Environ. Microbiol.*, 2013, 79, 4087–4093.
- 23 M. Zhang, P. Zheng, R. Wang, W. Li, H. Lu and J. Zhang, *Chemosphere*, 2014, 117, 604–609.
- 24 X. Li, L. Hou, M. Liu, Y. Zheng, G. Yin, X. Lin, L. Cheng, Y. Li and X. Hu, *Environ. Sci. Technol.*, 2015, 49, 11560–11568.
- 25 W. H. Yang, K. A. Weber and W. L. Silver, *Nat. Geosci.*, 2012, 5, 538–541.
- 26 M. Strous, E. Pelletier, S. Manganot, T. Rattei, A. Lehner, M. W. Taylor, M. Horn, H. Daims, D. Bartol-Mavel and P. Wincker, *Nature*, 2006, 440, 790–794.
- 27 R. Zhao, H. Zhang, Y. Li, T. Jiang and F. Yang, *Curr. Microbiol.*, 2014, 1–8.
- 28 B. Li, Y. Yang, L. Ma, F. Ju, F. Guo, J. M. Tiedje and T. Zhang, *ISME J.*, 2015, 9, 2490–2502.
- 29 T. Zhang, M.-F. Shao and L. Ye, *ISME J.*, 2011, 6, 1137–1147.
- 30 E. Isanta, T. Bezerra, I. Fernández, M. E. Suárez-Ojeda, J. Pérez and J. Carrera, *Bioresour. Technol.*, 2015, 181, 207–213.
- 31 Z.-r. Chu, K. Wang, X.-k. Li, M.-t. Zhu, L. Yang and J. Zhang, *Chem. Eng. J.*, 2015, 262, 41–48.
- 32 J. Guo, Y. Peng, L. Fan, L. Zhang, B. J. Ni, B. Kartal, X. Feng, M. S. Jetten and Z. Yuan, *Environ. Microbiol.*, 2015, DOI: 10.1111/1462-2920.13132.
- 33 D. R. Speth, S. Guerrero-Cruz, B. E. Dutilh and M. S. Jetten, *Nat. Commun.*, 2016, 7, 11172.
- 34 D. Emerson, E. J. Fleming and J. M. McBeth, *Annu. Rev. Microbiol.*, 2010, 64, 561–583.
- 35 J.-F. Gao, X. Luo, G.-X. Wu, T. Li and Y.-Z. Peng, *Bioresour. Technol.*, 2013, 138, 285–296.
- 36 D. Shu, Y. He, H. Yue, L. Zhu and Q. Wang, *Bioresour. Technol.*, 2015, 196, 621–633.
- 37 D. Shu, Y. He, H. Yue, L. Zhu and Q. Wang, *Bioresour. Technol.*, 2015, 186, 163–172.
- 38 P. Reichert, *Aquasim 2.0-user manual, computer program for the identification and simulation of aquatic systems*, Swiss Federal Institute for Environmental Science and Technology (EAWAG), 1998, vol. 219.
- 39 J. F. Andrews, *Biotechnol. Bioeng.*, 1968, 10, 707–723.
- 40 D. Shu, Y. He, H. Yue and Q. Wang, *Chem. Eng. J.*, 2016, 290, 21–30.
- 41 E. W. Rice, L. Bridgewater and A. P. H. Association, *Standard methods for the examination of water and wastewater*, American Public Health Association, Washington, DC, 2012.
- 42 M. E. Newman, *Proc. Natl. Acad. Sci. U. S. A.*, 2006, 103, 8577–8582.
- 43 Z. Bi, S. Qiao, J. Zhou, X. Tang and J. Zhang, *Bioresour. Technol.*, 2014, 170, 506–512.
- 44 S. C. Andrews, A. K. Robinson and F. Rodríguez-Quinones, *FEMS Microbiol. Rev.*, 2003, 27, 215–237.
- 45 N. Klüglein, F. Picardal, M. Zedda, C. Zwiener and A. Kappler, *Geobiology*, 2015, 13, 198–207.
- 46 W. Zhi, L. Yuan, G. Ji and C. He, *Environ. Sci. Technol.*, 2015, 49, 4575–4583.
- 47 V. M. Vadivelu, Z. Yuan, C. Fux and J. Keller, *Environ. Sci. Technol.*, 2006, 40, 4442–4448.
- 48 M. J. Kampschreur, R. Kleerebezem, W. W. de Vet and M. C. van Loosdrecht, *Water Res.*, 2011, 45, 5945–5952.
- 49 M. C. van Teeseling, R. J. Mesman, E. Kuru, A. Espaillet, F. Cava, Y. V. Brun, M. S. VanNieuwenhze, B. Kartal and L. van Niftrik, *Nat. Commun.*, 2015, 6, 1–10.
- 50 F. Ju, Y. Xia, F. Guo, Z. Wang and T. Zhang, *Environ. Microbiol.*, 2014, 16, 2421–2432.
- 51 A. Barberán, S. T. Bates, E. O. Casamayor and N. Fierer, *ISME J.*, 2012, 6, 343–351.
- 52 D. R. Lovley and E. J. Phillips, *Appl. Environ. Microbiol.*, 1988, 54, 1472–1480.
- 53 E. M. van den Berg, U. van Dongen, B. Abbas and M. C. van Loosdrecht, *ISME J.*, 2015, 9, 1–10.
- 54 M. Waki, T. Yasuda, Y. Fukumoto, K. Kuroda and K. Suzuki, *Bioresour. Technol.*, 2013, 130, 592–598.